X-ray photoelectron and static secondary-ion mass spectroscopic studies of segmented block copoly(ether–ester)s

Qamar S. Bhatia*† and Michael C. Burrell‡

**Polymer Materials Laboratory, and ‡Materials Characterization Laboratory, Corporate Research and Development, General Electric Company, Schenectady, New York 12301, USA*

(Received 22 February 1990; revised 18 June 1990; accepted 19 June 1990)

X-ray photoelectron spectroscopy (x.p.s.) and static secondary-ion mass spectroscopy have been applied to study the surface composition and structure of copoly(ether–ester) elastomers. These materials are multiblock copolymers containing repeat units that are capable of crystallization (hard segments) and amorphous blocks (soft segments). The hard segments in the samples examined were based on poly(butylene terephthalate) (PBT) and the soft block was poly(tetramethylene oxide) (PTMO). The results indicate that the surfaces of these copoly(ether–ester)s are always enriched in the soft segment and this enrichment is driven by the surface energy difference between the hard and soft segments. The surface enrichment is shown to vary with composition and molecular weight. For a copoly(ether–ester) containing 60% w/w PTMO in the bulk, average surface composition in the top 40 Å is seen to change from ~66% w/w for PTMO of $M_n = 1000$, to ~85% for PTMO of $M_n = 2900$. Differential scanning calorimetry studies in conjunction with x.p.s. studies suggest that the surface enrichment is reduced by an increase in the bulk crystallinity of the material. Addition of poly(hexamethylene terephthalate) to the PBT hard segment reduces the bulk crystallinity of the copoly(ether–ester)s and results in a surface that is more enriched in the PTMO soft segment. The process by which the sample is prepared is also shown to affect the extent of surface enrichment. The angle-dependent x.p.s. data have been fitted by a continuous profile, which shows an enriched soft-segment region at the air/copolymer interface and a depleted region adjacent to the preferentially enriched surface layer.

(Keywords: spectroscopy; block copolymers; surface composition)

INTRODUCTION

The copoly(ether–ester) thermoplastic elastomers are multiblock copolymers containing repeat units that are capable of crystallization (hard segments) and amorphous blocks (soft segments). At service temperature the partially crystallized hard segments act as physical crosslinks, but at processing temperatures the crystallites melt leading to the thermoplastic behaviour. The ease of processability and excellent mechanical properties of these copolymers have led to their extensive use as a replacement for vulcanized rubber, coverings for wire and optical fibre cables and for numerous automotive uses[1]. The commercial copoly(ether–ester) elastomers consist of a polyester hard segment, e.g. poly(butylene terephthalate) (PBT), and a polyether soft segment, e.g. poly(tetramethylene oxide) (PTMO) or poly(propylene oxide) (PPO). The bulk morphology[2–9], mechanical properties[6,10] and melt rheology[10–13] of copoly(ether–ester) elastomers have been studied in some detail; however, little is known about their surface structure and properties. Better understanding of the surface structure and properties is critical for controlling properties such as adhesion, friction, weatherability and paintability of these materials.

X-ray photoelectron spectroscopy (x.p.s.) has proved to be the most valuable tool for quantitative characterization of polymer surfaces. The photoemission spectra obtained in an x.p.s. experiment can provide a quantitative measure of the surface chemical composition. In addition, the use of angle-dependent x.p.s. can provide information on the inhomogeneity in the surface composition and structure in the top 15–70 Å of the polymer. X.p.s. has been applied to a variety of block copolymers[14–20] and polyblends[21,22] to document the surface enrichment and structure. Recently, static secondary-ion mass spectroscopy (s.s.i.m.s.) has emerged as a valuable complementary technique to x.p.s. for fully characterizing a polymer surface. S.s.i.m.s. can provide greater molecular specificity with very high sensitivity: the sampling depth has been shown[23] to be 8–12 Å. Briggs and coworkers[24–26] have done extensive work in applying s.s.i.m.s. in various aspects of polymer surface analysis. X.p.s. and s.s.i.m.s. studies of polyurethanes[27,28] are of particular relevance to this work.

The surface segregation in copolymers is governed by a variety of factors. There is a thermodynamic driving force for minimizing the total free energy of the system, which results in the preferential surface adsorption of the lower-surface-energy constituent of the copolymer. However, a number of other factors prevent the surface from attaining a thermodynamic equilibrium. These factors could be extrinsic, such as the type of solvent used or the rate at which the solvent is evaporated, or dependent on the sample preparation method. Intrinsically, the relative length of the blocks, their sequence length distribution and the concentration of the constituents may play a crucial role in determining the surface of a copolymer. If one of the components is crystallizable,

† Present address: GE Plastics, 1 Noryl Avenue, Selkirk, NY 12158, USA

0032-3861/91/111948-09

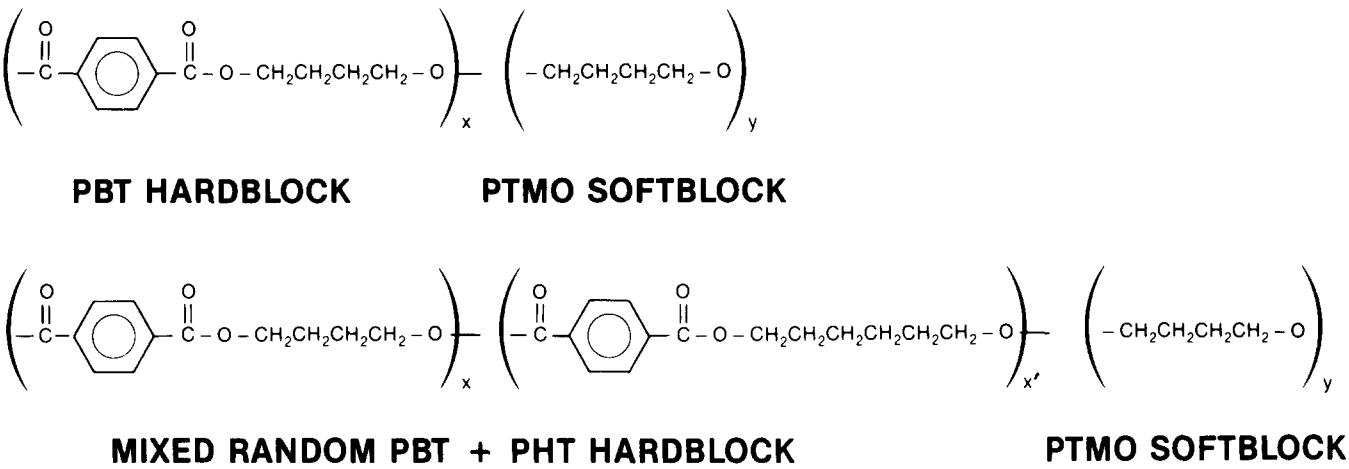

Figure 1 Chemical structure of PBT–PTMO copoly(ether–ester)s

the kinetics and morphology of crystallization may play a dominant role.

In the present report, x.p.s. and s.s.i.m.s. have been employed to quantify the surface composition and gradient of multiblock poly(ester–ether) copolymers based on PBT and PTMO as a function of composition and molecular weight of soft segment. Surface studies on PPO soft-segment-based copoly(ether–ester)s have been reported in another paper[29].

EXPERIMENTAL

Materials

The copoly(ether–ester)s are prepared by the melt transesterification of dimethylterephthalate (DMT), 1,4-butanediol and poly(tetramethylene ether) glycol following a procedure described by Witsiepe[30] and Hoeschele[31]. Glycols of number-average molecular weight $M_n = 1000$, 2000 and 2900 were used. The resultant polymer, shown in *Figure 1*, consists of randomly joined PTMO soft segments and sequences of butylene terephthalate hard segments. The final copolymer has an expected geometric molecular-weight distribution, with M_n being approximately 25 000–30 000. Addition of hexanediol (HD) during the polymerization reaction leads to a hard-segment block consisting of random PBT and poly(hexamethylene terephthalate) (PHT) sequences. Here we use the following code: the H(30) specimen indicates a PBT/PHT hard block with a 70/30 mole ratio. An example of the nomenclature followed gives H(30)54/S(1) as a PBT/PHT hard segment containing 30 mol% PHT, a total hard-segment content of 54% by weight, and the rest consists of PTMO soft segment of $M_n = 1000$. In copolymers with PTMO of $M_n = 2000$ the S(2) symbol is not used and the resulting specimen symbol is H(30)54. The characteristics and symbols of specimens studied are given in *Table 1*.

Sample preparation

The pellets of copoly(ether–ester)s obtained were washed in hexane before making solutions. The x.p.s. samples were studied as spin-cast and solvent-cast films and also as moulded plaques. The films of the copolymers were prepared by spin coating a 2–4% w/w solution of the copolymer in chloroform(90)/*m*-cresol(10) mixed solvent onto microscope coverslips. Spin coating of the films was done at 1000 rpm for a time period of 40 s. Samples were also prepared as solvent-cast films from chloroform(90)*m*-cresol(10) and hexafluoroisopropanol (HFIP) solvent. The films were dried under a hood at room temperature for 24 h, before annealing in a vacuum oven at 100°C for varying periods of time. The plaques were injection moulded with barrel temperatures of 200°C for H(30) specimens, with the mould temperature of 80°C.

Table 1 Characteristics of copoly(ether–ester) specimens

Copolymer	Bulk weight per cent of hard segment	Hard-segment mole ratio PBT/PHT	Molecular weight of soft segment
H(0)43/S(1)	43	100/0	1000
H(0)60/S(1)	60	100/0	1000
H(0)72/S(1)	72	100/0	1000
H(0)83/S(1)	83	100/0	1000
H(0)23/S(2)	23	100/0	2000
H(0)29/S(2)	29	100/0	2000
H(0)40/S(2)	40	100/0	2000
H(0)50/S(2)	50	100/0	2000
H(0)40/S(2.9)	40	100/0	2900
H(30)75/S(2)	75	70/30	2000
H(30)65/S(2)	65	70/30	2000
H(30)59/S(2)	59	70/30	2000
H(20)59/S(2)	59	80/20	2000
H(30)54/S(2)	54	70/30	2000
H(20)54/S(2)	54	80/20	2000

Instrumentation

X.p.s. spectra were recorded with a Surface Science Laboratories SSX-100 spectrometer using a monochromatized Al Kα source irradiating an area on the sample of 600 μm^2. The analyser was operated at a pass energy of 50 eV for high-resolution scans and 150 eV for survey scans. The surface charging that occurred due to the non-conductive nature of the samples was neutralized with 1–2 eV low-energy electrons from an electron flood gun. The binding energy of the C_{1s} signal from hydrogen–carbon at 284.6 eV was used as an internal calibration of the absolute binding energy scale.

The integrated intensity I_i of a core-electron photoemission spectrum is given by:

$$I_i = N_i S_i \quad (1)$$

where N_i is the average number of atoms per unit

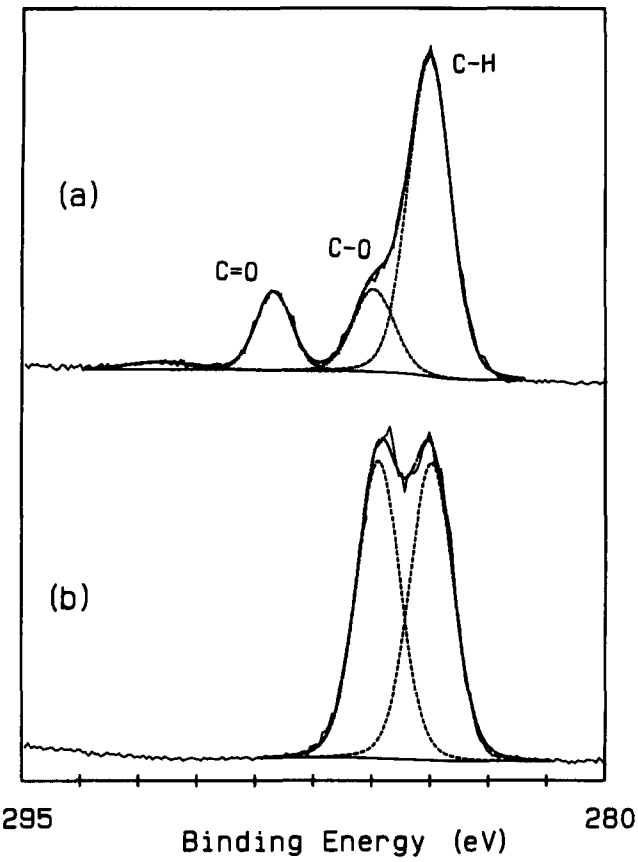

Figure 2 High-resolution C_{1s} x.p.s. spectra of (a) PBT and (b) PTMO

Table 2 Characteristics of x.p.s. core levels for the homopolymers

Homopolymer	Peak	Binding energy (eV)	Width (eV)
PBT			
C_{1s}	C–H	284.6	1.3
	C–O	286.1	1.2
	C=O	288.6	1.0
	Shake-up	291.6	1.9
O_{1s}	C=O	531.7	1.4
	C–O	533.2	1.4
PTMO			
C_{1s}	C–H	284.6	1.1
	C–O	286.0	1.1
O_{1s}	C–O	532.3	1.5

sampling volume and S_i is the sensitivity factor of element i. The sensitivity factors take into account the kinetic energy dependence of the inelastic mean free path of emitted electrons and the photoelectron cross-section[32]. A quantitative elemental analysis can be achieved by taking the ratio of the measured x.p.s. intensities. Quantification of the soft-segment (or hard-segment) content at the surface is accomplished by resolving the component peaks in the C_{1s} signal. This relies on a curve-fitting procedure with an estimated error of $\pm 5\%$, resulting in a maximum error of 2 wt% in the surface composition. All the data were analysed using the standard software provided with the SSX-100 instrument.

The s.i.m.s. experiments were done at a Physical Electronics Laboratory (Eden Prairie, MN) on a 6300 SIMS system or a 5400 ESCA/SIMS system. The primary ion source was 4 kV Xe^+ operated at a current of 60 pA. Total ion dose during the measurement of the secondary-ion spectrum was $< 10^{13}\,cm^2$.

X-RAY PHOTOELECTRON SPECTROSCOPY RESULTS

Homopolymers

The C_{1s} spectra for PBT and PTMO are shown in *Figure 2*. The C_{1s} peak for PBT (*Figure 2a*) contains contributions from carbon–hydrogen (at 284.6 eV), carbon–oxygen (at 286.0 eV), the ester carboxyl group (at 288.6 eV) and a shake-up peak accompanying the photoemission from the aromatic rings (at 291.6 eV). The PTMO sample was of molecular weight 2000 and was in the form of a viscous liquid spread over a microscope coverslip. The PTMO peak spectrum (*Figure 2b*) is a doublet comprising the carbon–hydrogen and carbon–oxygen peaks. Characteristics of the C_{1s} x.p.s. peaks for homopolymers are given in *Table 2*.

Copolymers

The C_{1s} photoelectron x.p.s. spectra at take-off angle = 35° for the solvent-cast copolymer films as a function of composition and molecular weight of soft segments are shown in *Figure 3*. The C–H and C–O peaks contain contributions from both the PBT hard segment and the PTMO soft segment, while the carboxyl peak in the spectra arises solely from PBT present in the surface region. Using equation (1) and assuming that C in all the chemical environments has the same sensitivity factor, we obtain the expression for obtaining the weight

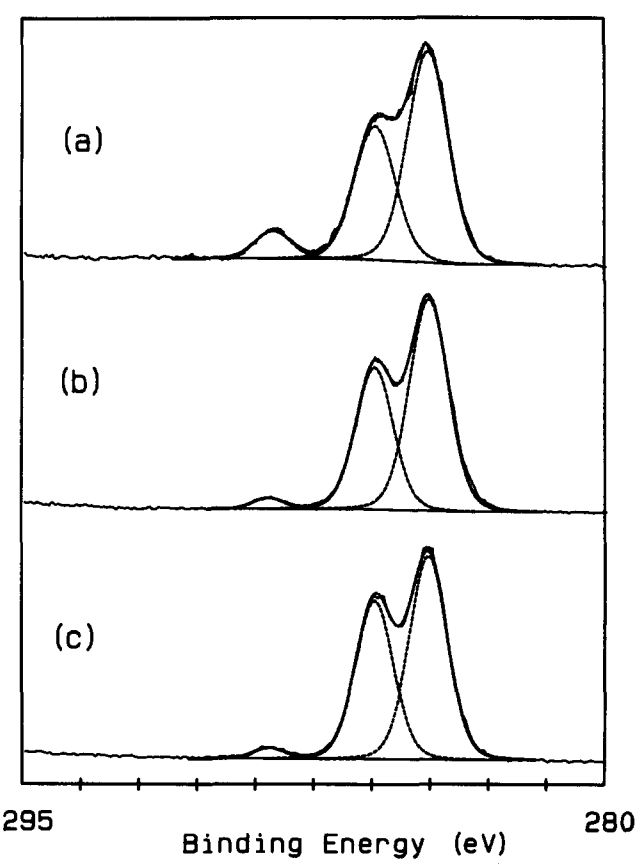

Figure 3 High-resolution C_{1s} x.p.s. spectra for copoly(ether–ester)s: (a) H(0)43/S(1), (b) H(0)40 and (c) H(0)40/S(2.9) (take-off angle = 35°)

per cent of soft segment at the surface as:

$$w_s = (R-1)/(R+2.055) \quad (2)$$

where w_s is the average weight fraction of the soft segment within the sampling depth of x.p.s. By measuring the area intensity ratio $R = I(\text{C–O})/I(\text{C=O})$ from x.p.s. C_{1s} spectra, the weight per cent of the soft segment at the surface of copoly(ether–ester)s can be calculated. Equation (2) has to be modified slightly for analysing the PBT/PHT hard-segment copoly(ether–ester)s. The average surface weight per cent of PTMO is plotted as a function of the bulk composition for various samples examined in *Figure 4*. A significant surface enrichment of the PTMO soft block is evident, e.g. for H(30)54, which contains 46% PTMO in the bulk, the top 40 Å has an average composition of ~80% soft block. The relative amount of surface enrichment is represented by the distribution coefficient for PTMO defined as:

$$K = (\text{surface wt\% PTMO})/(\text{bulk wt\% PTMO}) \quad (3)$$

The distribution coefficients are given in *Table 3* and are seen to be inversely related to the bulk PTMO content. For the same bulk composition, higher M_n soft segments show a higher enrichment factor. As is indicated in *Table 3*, the sample preparation method affects the relative surface enrichment. The moulded plaques give a lower surface enrichment than the spin-cast or solvent-cast films.

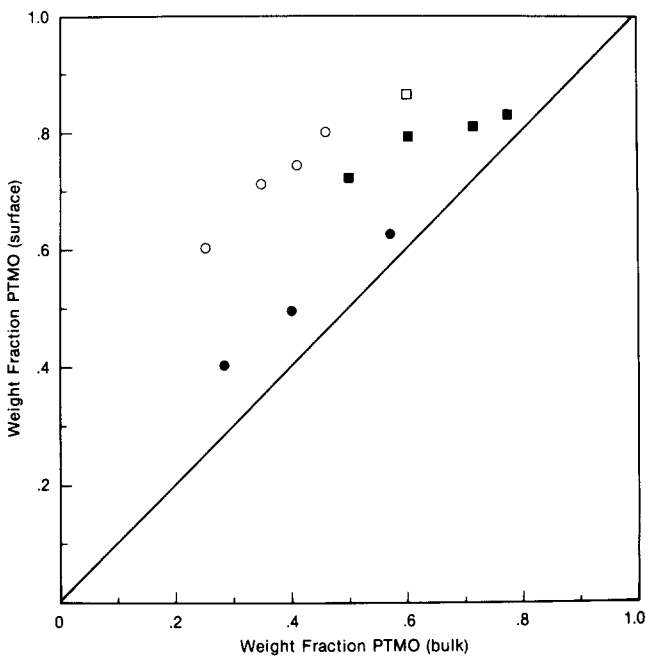

Figure 4 Surface weight fraction PTMO *versus* bulk weight fraction for various copoly(ether–ester)s: (●) H(0)S(1); (○) H(30)S(2); (■) H(0)S(2); (□) H(0)S(2.9)

Table 3 X.p.s. distribution coefficients for H(30)S(2) copoly(ether–ester)s

Copolymer	Moulded	Solvent-cast	Spin-cast
H(30)54	1.71	1.62	1.69
H(30)59	1.8		
H(30)65	2.04	1.92	2.11
H(30)75	2.4		

STATIC SECONDARY-ION MASS SPECTROSCOPY RESULTS

Homopolymer spectra

The positive-ion s.s.i.m.s. spectrum of PTMO is shown in *Figure 5*. Our s.s.i.m.s. data for PTMO agree well with previously reported spectra obtained in studies of poly(ether urethane)s[28]. The PTMO spectrum shows the most intense peaks at $m/e = 55$, 71 and 73. Several possible ion structures may be proposed for each characteristic peak[28], and some representative structures are shown in *Figure 5*. The positive-ion s.i.m.s. spectrum of PBT is shown in *Figure 6*. In the low-mass region the spectrum shows the $C_nH_m^+$ fragments, with the largest peak at $m/e = 55$ ($C_4H_7^+$). The remainder of the spectrum is similar to poly(ethylene terephthalate) (PET)[26] with characteristic peaks at $m/e = 76$, 91, 104 and 149. In the case of H(30) specimens the positive s.i.m.s. fragmentation pattern for the hard block is not expected to be different from that of H(0) specimens.

Copolymer spectra

The spectrum for the copolymers contains a combination of fragments from the constituent homopolymers. A typical spectrum for copoly(ether–ester)s is given in

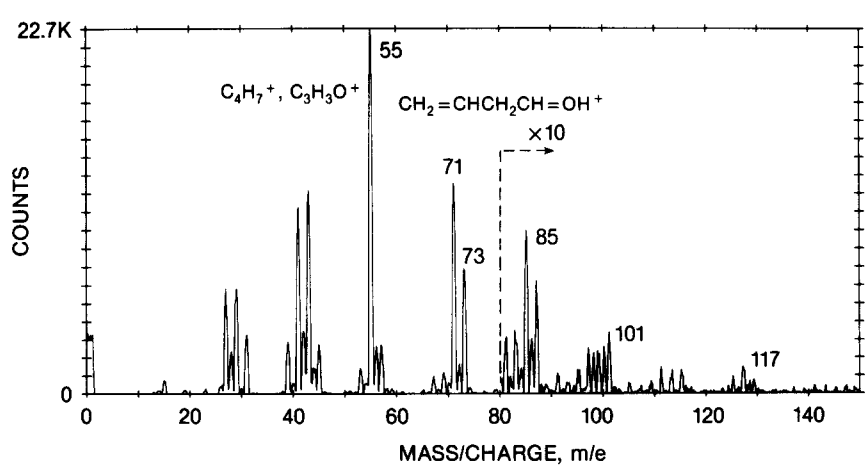

Figure 5 Positive-ion s.s.i.m.s. spectrum of PTMO

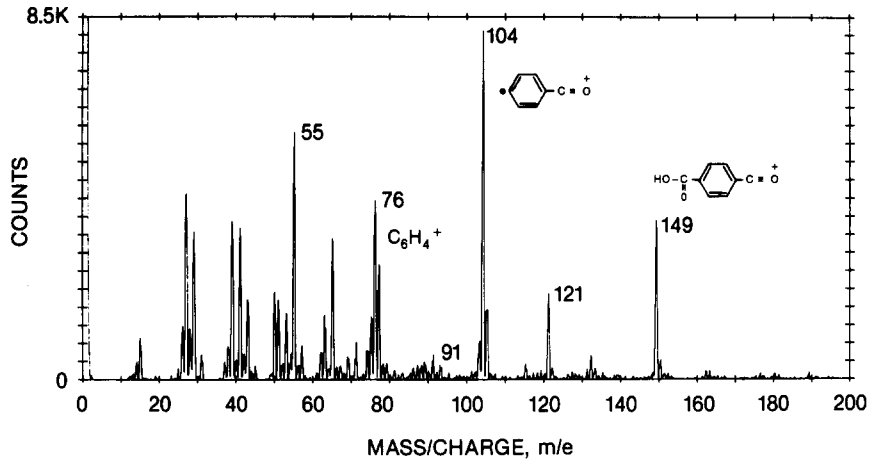

Figure 6 Positive-ion s.s.i.m.s. spectrum of PBT

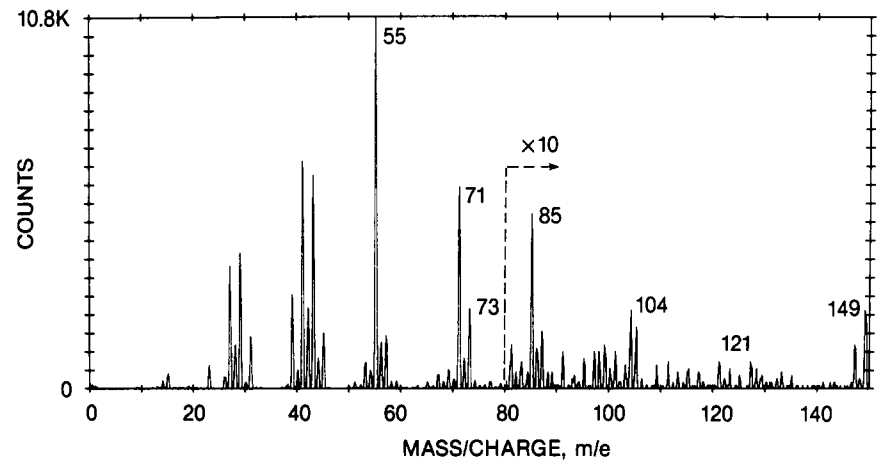

Figure 7 Positive-ion s.s.i.m.s. spectrum of H(30)54 copoly(ether–ester)

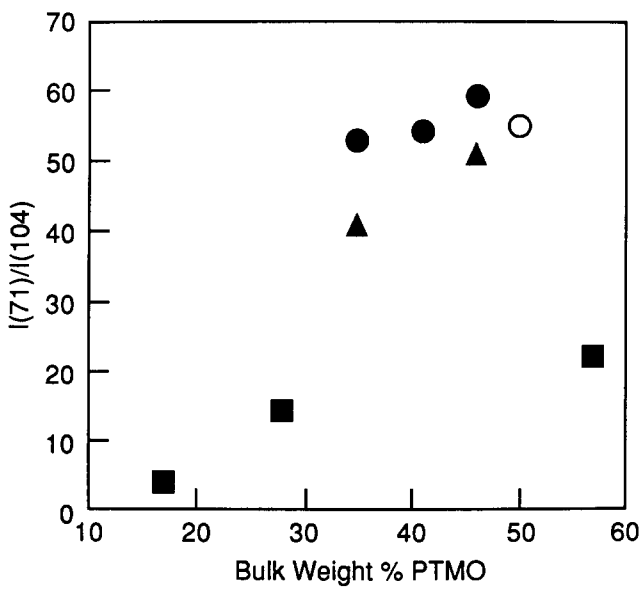

Figure 8 Ratio of $I(71)/I(104)$ ion peaks: (●) H(30)S(2) films; (▲) H(20)S(2) plaques; (■) H(0)S(1) films; (○) H(0)S(2) films

Figure 7. In general, the major peaks arise from the soft segment, consistent with PTMO-enriched surface layer determined from x.p.s. The presence of PBT at the surface probed by the s.i.m.s. technique indicates that the surfaces are not purely soft segment. This information is not obtainable from x.p.s. measurements, which sample a larger depth (~20 Å).

Although s.s.i.m.s. is not easily quantifiable, it is reasonable to expect that the relative characteristic ion intensities for a multicomponent polymer are related to the amounts of the individual constituents. *Figure 8* gives the $I(71)/I(104)$ ratio for the various PTMO-based copolymers. The results suggest that the soft-segment composition at the surface increases with increasing bulk content of the soft segment. The samples consisting of soft segment of $M_n = 1000$ show a much lower ratio than the samples containing $M_n = 2000$ soft segment. For the case of the H(30) specimen, the plaques show a lower degree of surface enrichment compared to the solvent-cast films, as was evident from the x.p.s. data. More extensive s.s.i.m.s. studies of copoly(ether–ester)s having mixed polyether soft segments have been reported elsewhere[33].

DISCUSSION

The surfaces of all the copoly(ether–ester) samples examined showed surface enrichment of the lower-surface-energy soft block. The surface composition goes up with an increase in the bulk composition. However, the relative surface enrichment given by the distribution coefficients for the soft blocks is inversely related to the bulk formation. The driving force for the surface

enrichment is the surface energy difference between the constituent blocks. The surface energy of the PBT and PBT/PHT hard blocks[34] is $\sim 44\,dyn\,cm^{-1}$ and of the PTMO soft blocks[35] is $\sim 32\,dyn\,cm^{-1}$. A variety of other factors, however, influence the extent of surface enrichment of the soft block. From our results on the H(0) samples it is obvious that the length (i.e. molecular weight, MW) of the soft block plays a significant role. For a H(0) copoly(ether–ester) containing 60% w/w PTMO in the bulk, the corresponding surface composition goes from $\sim 66\%$ for PTMO of $MW = 1000$ to $\sim 80\%$ for PTMO of $MW = 2000$ and $\sim 86\%$ for PTMO of $MW = 2900$. The longer block length of the soft segment makes it configurationally easier for it to orient at the surface. The block length effect on the surface enrichment in block copolymers has been previously documented for poly(ethylene oxide)/poly(propylene oxide) (PEO/PPO)[31], poly(butyl acrylate)/poly(dimethylsiloxane) (PBAC/PDMS)[17], polysulphone/PDMS[18] and for polyurethanes[19].

The bulk morphology of these copoly(ether–ester)s exhibits a two-phase structure consisting of a crystalline phase made up of PBT and an amorphous phase made of the uncrystallized PBT and the non-crystallizable polyethers[2–8]. The crystalline regions physically crosslink the amorphous phase and should inhibit the soft segment from preferentially migrating to the surface. As the bulk crystallinity of the material increases, the concentration of the physical crosslinks increases, thus making it configurationally harder for the soft segment to orient at the surface. The increase in molecular weight of the soft block reduces the weight fraction of crystallized PBT and the overall crystallinity in the copoly(ether–ester)s, as has been shown by Wegner *et al.*[36] using d.s.c.

The incorporation of the hexanediol (HD) in the PBT hard-segment copolymer reduces the melting point and the amount of crystallinity in these materials as compared to the copolymers that have a pure PBT hard segment[3]. A copoly(ether–ester) with a hard segment of 50 wt% PBT is compared to a H(30) that has ~ 54 wt% hard segment. D.s.c. results give the heat of fusion for copolymer H(30)54 as $\sim 30\%$ lower than that of the H(0)50 specimen, and melting temperatures of 156 and 213°C respectively. The crystalline weight fraction of these samples can be estimated as:

$$w_c = \Delta h / \Delta h_{PBT} \qquad (4)$$

where Δh_{PBT} is the heat of fusion of fully crystalline PBT, which is taken[8] as $140.5\,J\,g^{-1}$. The resulting crystalline weight fractions are 0.182 and 0.138, respectively, for the H(0)50 and H(30)54 samples. The x.p.s. results show that the less crystalline material H(30)54 has a distribution coefficient $K = 1.74$ while the more crystalline H(0)50 has $K = 1.44$. The H(20)54 sample with 20% HD content has a crystalline weight fraction of 0.15 and the corresponding enrichment factor is $K \simeq 1.58$ as shown in *Table 4*. Similar results are also obtained for the H(30)59 and H(20)59 samples. Reduction in the hexanediol content from 30 to 20% is shown to reduce the surface composition of the respective copolymers from $\sim 76\%$ to $\sim 71\%$ soft segment.

Table 4 Effect of hexanediol on the surface composition of copoly(ether–ester)s

Copolymer	w_c	K
H(30)54	0.138	1.74
H(20)54	0.15	1.58
H(0)50	0.182	1.44

Annealing above the glass transition of PBT (~ 40°C) is expected to increase the crystallinity of the copoly(ether–ester); however, it shows little effect on surface enrichment. This is not surprising as, once the surface has been enriched, further annealing increases the crystallinity, making it morphologically harder for any further surface enrichment, but it is thermodynamically unfavourable for the soft segment to migrate back into the bulk. This is further corroborated by the results on the melt-quenched H(30)75 specimen. An almost amorphous copoly(ether–ester) results after quenching the melted copoly(ether–ester) in liquid nitrogen. There is very little morphological constraint on the polyether segment to adsorb preferentially to the surface, and thus the resulting surface composition is highly enriched ($\sim 82\%$ by weight PTMO within the x.p.s. sampling depth). Further annealing of the sample at 100°C showed very little change in the surface composition. More detailed studies on the effect of bulk crystallinity on surface composition of these copoly(ether–ester)s is being undertaken.

As is obvious from the x.p.s. results the method by which the sample is prepared has a significant effect on the resulting surface composition. This is illustrated in *Table 3* by the varying surface enrichments obtained depending on the solvent-cast, spin-cast, or moulded plaque samples. This result is confirmed by s.s.i.m.s. results for the films and plaques. The type of solvent used to cast the films also has an effect on surface enrichment. Use of a solvent that has an affinity for one of the components will result in that moiety being preferentially adsorbed on the surface. A chloroform(90)/*m*-cresol(10) mixture and HFIP solvents were used to cast films of H(30)54 copolymer. HFIP is a better solvent for PBT and this results in a lowering of surface composition of PTMO by ~ 4 wt% for the film cast from this solvent.

The effects of the copoly(ether–ester) molecular-weight distribution and the hard-segment sequence-length distribution on the surface enrichment have not been explicitly addressed in this study. However, it is important to discuss the consequences of these effects, which result from the structure of these multiblock copolymers. Previous surface studies on bimodal molecular-weight blends have failed to document any surface fractionation according to MW[37]. Recent lattice model calculations[38] have shown that the fractionation is of the order of $< 1\%$. The hard-segment distribution, however, can have a substantial effect on the resulting surface of the copoly(ether–ester). The block-length distribution resulting from a truly random polycondensation reaction is given by Frensdorff[39]. A significant portion of the PBT blocks contain less than the average hard-segment length. A consequence of the presence of PBT blocks having very small block lengths is the joining of two soft segments without the possibility of a tie point existing between them. The resulting soft-segment length is greater than the length of the PTMO glycol. As has been shown in this study, the higher M_n of soft segment should facilitate the soft segment to orient at the surface. Additionally, Perego *et al.*[9] have shown that PBT of block length less than three units does not crystallize. These short PBT chains, which are amorphous, are more likely to migrate to the surface. Quantitative measures

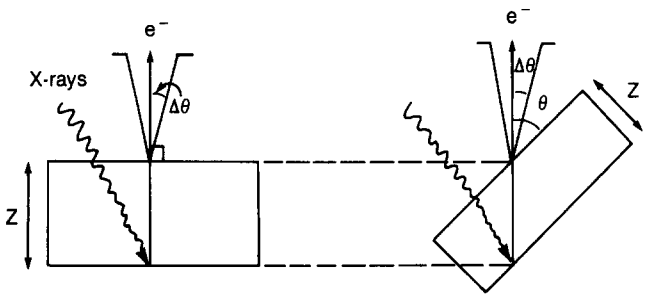

θ	Z(Å)
90	75
55	61
35	45
25	35
15	26

Figure 9 Schematic of a.d.x.p.s. experiment for depth profiling, and the corrected sampling depths

of these effects are difficult to ascertain from this study. Model compounds with known block-length distribution could be studied with x.p.s. to get a better understanding of these effects.

ANGLE-DEPENDENT X-RAY PHOTOELECTRON SPECTROSCOPY

Angle-dependent x.p.s. (a.d.x.p.s.) is a method to probe surface inhomogeneity in the top 20–70 Å of a multi-component polymer. The x.p.s. intensity of a given core level at a take-off angle θ (see *Figure 9*) is given by:

$$I_i = K(\theta)\int_0^\infty C(z)\exp(-z/\lambda\sin\theta)\,dz \qquad (5)$$

where K is the product of the sample and instrument sensitivity factors for a given analysis geometry and $C(z)$ is the concentration of element i at depth z. The sampling depth of x.p.s. is limited by the effective mean free path λ for electrons escaping from the surface. Accurate knowledge of the electron mean free path is vital to the quantitative success of x.p.s. depth profiling; however, there is considerable discrepancy in the literature values for λ. We have chosen the value of $\lambda \sim 25$ Å as was obtained experimentally by Clark *et al.*[40] and Szajman *et al.*[41]. At take-off normal to the surface, the effective sampling depth is a maximum. The effective sampling depth can be decreased according to:

$$z = 3\lambda\sin\theta \qquad (6)$$

For the SSX-100, the analyser lens collects photo-electrons with an aperture of 30°, making the instrument less surface-sensitive at grazing angles. Correction procedures have been developed to ascertain the correct sampling depth[42] and these are tabulated in *Figure 9*.

In practice, to infer the surface morphology of a multi-component polymer from angle-dependent x.p.s. data, a model can be assumed for the surface morphology and then checked for its validity. The composition variation $C(z)$ corresponding to the assumed model is substituted in equation (5) and the intensity obtained by the resulting integration is compared with the experimentally obtained x.p.s. intensity. Different surface morphologies have been suggested for block copolymer surfaces. The substrate–overlayer model has an enriched surface layer atop the bulk composition layer, as has been observed in many PDMS-containing copolymers[14]. Cylindrical domains oriented perpendicular to the surface have been inferred from a.d.x.p.s. results obtained on polystyrene/poly-(ethylene oxide) (PS/PEO)[15,16] and polycarbonate/poly-(dimethylsiloxane) (PC/PDMS)[18]. Transmission electron microscopy studies on polystyrene/polybutadiene (PS/PB)[43,44] have suggested an alternating lamellar morphology both perpendicular and parallel to the free surface. Fredrickson[45] has shown that block copolymers can possess oscillatory surface composition profiles because of the connectivity of the constituent blocks and the amplitude of these oscillations is exponentially damped in the bulk. A depletion layer adjacent to the preferentially adsorbed surface layer in block copolymers has also been predicted by a lattice model developed by Theodorou[46]. The surface concentration profile in a block copolymer is given as[45]:

$$C(z) = C(b) + [C(0) - C(b)]\exp(-z/\xi)\cos(\Omega z) \qquad (7)$$

where ξ is related to the bulk correlation length, Ω is the wavenumber of the oscillation and $C(0)$ is the weight fraction at the air/copolymer interface. These oscillatory profiles have been confirmed experimentally for polystyrene/poly(methyl methacrylate) (PS/PMMA) block copolymer films by the neutron reflection technique[47].

Angle-dependent x.p.s. experiments were performed to obtain the non-destructive surface composition–depth profile of H(30) copolymers. Representative angle-dependent C_{1s} core-level x.p.s. spectra at angles 15°, 35° and 90° are shown in *Figure 10*. Analysis of the data

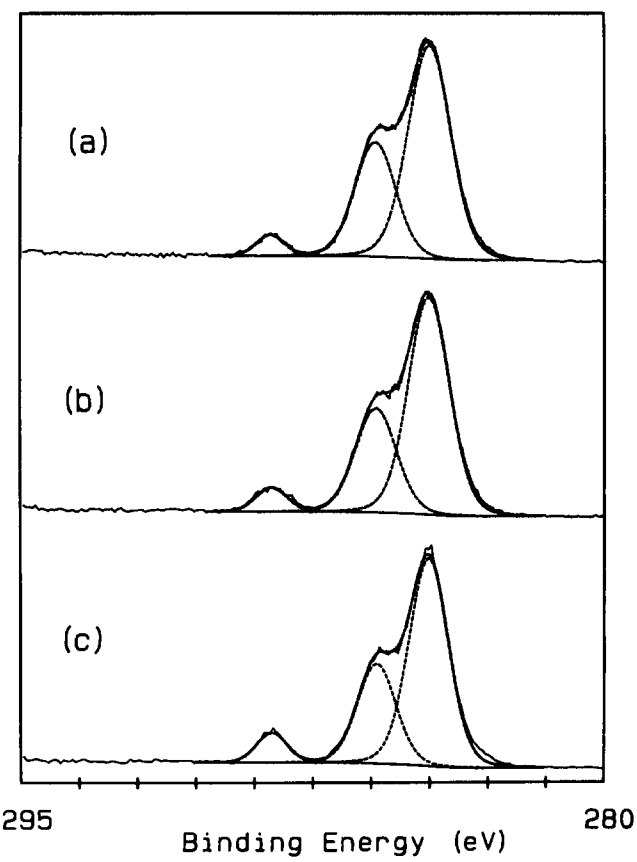

Figure 10 Angle-dependent C_{1s} x.p.s. spectra for H(30)75 film at angles of (a) 15°, (b) 35° and (c) 90°

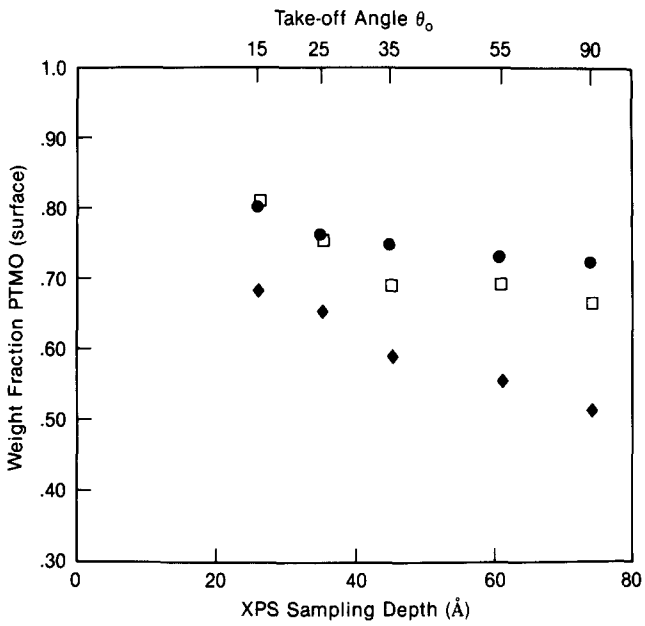

Figure 11 Surface composition as a function of sampling depth for copoly(ether–ester)s: (●) H(30)54; (□) H(30)65; (◆) H(30)75

according to equation (2) at each angle gives the average surface composition as a function of the effective sampling depth. *Figure 11* shows the surface composition as a function of the sampling depth for H(30)54, H(30)65 and H(30)75. There is a concentration gradient in the three copolymers; however, H(30)25 shows the steepest profile as the average surface weight per cent of PTMO drops from ~68% in the top 20 Å to ~50% in the top 70 Å. The H(0) copoly(ether–ester) films show a lesser angular dependence in their C_{1s} intensities.

Angle-dependent x.p.s. data obtained on the copoly(ether–ester) have been tested for different models that have been suggested. The results do not suggest a domain morphology. The substrate–overlayer model or a continuous profile are more likely to fit the a.d.x.p.s. data obtained on these materials. The substrate–overlayer model has two parameters, the composition and thickness of the overlayer. For an overlayer of thickness d, the intensities for C–O can be written as:

$$I_o(\text{C–O}) = S(\theta_0)N_o(\text{C–O})\int_\theta T(\theta,\theta_0) \times [1-\exp(-d/\lambda\sin\theta)]\,d\theta \quad (8a)$$

and for the substrate as:

$$I_s(\text{C–O}) = S(\theta_0)N_s(\text{C–O})\int_\theta T(\theta,\theta_0)\exp(-d/\lambda\sin\theta)\,d\theta \quad (8b)$$

where S and T are the sensitivity factors and collection angle distribution function[42]. Similar expressions can be written for I(C=O). The integrals are necessary to account for the finite angular acceptance of the analyser lens. Using these equations, the expected I(C–O)/I(C=O) ratios, as a function of the experimental take-off angle θ_0, can be obtained. We have also modelled the profile given by expression (7) to compare with the experimentally obtained intensities.

Figure 12 presents the resultant x.p.s. profiles for H(30)75, using the two models described above. The predicted variation in the x.p.s. composition (broken curve in *Figure 12*) with depth for the substrate–overlayer model is somewhat steeper than the experimentally measured compositions. There is better agreement between the experimental data and the predicted values derived from the continuous profile given by equation (7). A good fit is obtained for the H(30)75 cast film, using a correlation length of 25 Å and a wavenumber of 2.5 $Å^{-1}$. Equally reasonable fits to the a.d.x.p.s. experimental data were also obtained for H(30)65 and H(30)54 copolymer films. The fits of the experimental data could be obtained with numerous combinations of the model parameters (ξ,Ω). This modelling points out the weakness of x.p.s. as a technique to infer the exact composition profile. The integration carried out in equation (5) makes the resultant intensities less sensitive to model parameters. An enriched overlayer over a substrate of bulk composition is a good approximation for the continuous profile for fitting the a.d.x.p.s. data.

CONCLUSIONS

A systematic x.p.s. and s.s.i.m.s. study of surfaces of PBT–PTMO multiblock copolymers has been carried out. The results show that the copoly(ether–ester) surface always shows an enrichment of the PTMO soft segment. This preferential adsorption is driven by the surface energy difference between the hard and soft segments. The relative surface enrichment is seen to decrease with increasing bulk content, and increases with increasing M_n of the soft segment. Surface enrichment decreases as the overall bulk crystallinity of the sample increases. This is shown by comparing the surface compositions of copoly(ether–ester) with addition of hexanediol in the PBT hard segment. Surface enrichment is also shown to depend on the process by which the surface is prepared. The a.d.x.p.s. data are fitted by a continuous profile, which gives an enriched soft-segment layer at the

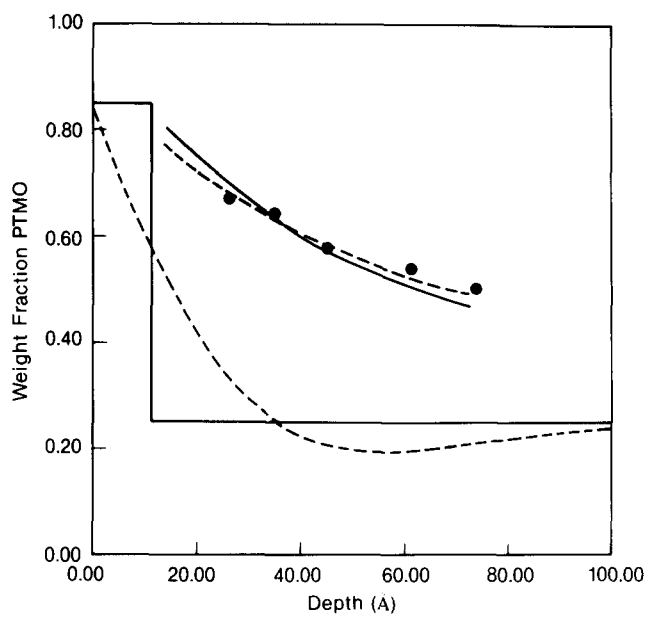

Figure 12 The measured a.d.x.p.s. data points (●) for H(30)75 copoly(ether–ester). The composition profile obtained from the substrate–overlayer model (——) and the continuous profile of equation (7) (-----) are the lower traces. The corresponding integrated a.d.x.p.s. profiles obtained from equation (5) are the upper traces

air/copolymer interface and a depleted region adjacent to it because of the chemical linkage. The substrate–overlayer model is a good approximation for the profile.

ACKNOWLEDGEMENTS

The authors wish to acknowledge G. F. Smith of GE Plastics and G. K. Hoeschele of DuPont Experimental Station for supplying the specimens studied and Al Shultz for the d.s.c. measurements. Useful discussions with M. Takemori of GE CRD, and R. Allen and R. Michael of GE Plastics are appreciated.

REFERENCES

1 Legge, N. R., Holden, G. and Schroeder, H. E. (Eds.) 'Thermoplastic Elastomers: A Comprehensive Review', Hanser, New York, 1987, Chs. 8 and 13
2 Cella, R. J. *J. Polym. Sci., Polym. Symp.* 1973, **42**, 727
3 Ghaffar, A., Goodman, I. and Hall, I. H. *Br. Polym. J.* 1973, **5**, 315
4 Shen, M., Mehra, U., Niinomi, M., Koberstein, J. T. and Cooper, S. L. *J. Appl. Phys.* 1974, **45**, 4182
5 Seymour, R. W., Overton, J. R. and Corley, L. S. *Macromolecules* 1975, **8**, 331
6 Lilaonitkul, A., West, J. C. and Cooper, S. L. *J. Macromol. Sci–Phys. (B)* 1976, **12** (4), 563
7 Zhu, L. L. and Wegner, G. *Makromol. Chem.* 1981, **182**, 3625
8 Bandara, U. and Droscher, M. *Colloid Polym. Sci.* 1983, **261**, 26
9 Perego, G., Cesari, M. and Vitali, R. *J. Appl. Polym. Sci.* 1985, **29**, 1157
10 Walker, B. W. 'Handbook of Thermoplastic Elastomers', Van Nostrand Reinhold, New York, 1979
11 Lilaonitkul, A. and Cooper, S. L. *Rubber Chem. Technol.* 1977, **50**, 1
12 Brown, M. and Witsiepe, W. K. *Rubber Age* 1972, **104**, 35
13 Hoeschele, G. K. and Witsiepe, W. K. *Angew. Makromol. Chem.* 1973, **29**, 267
14 Clark, D. T., Peeling, J. and O'Malley, J. J. *J. Polym. Sci., Polym. Chem. Edn.* 1976, **14**, 543
15 Thomas, H. R. and O'Malley, J. J. *Macromolecules* 1979, **12**, 323
16 O'Malley, J. J., Thomas, H. R. and Lee, G. M. *Macromolecules* 1979, **12**, 966
17 McGrath, J. E., Dwight, D. W., Riffle, J. S., Davidson, T. F., Webster, D. C. and Vishwanathan, R. *Polym. Prepr., ACS Div. Polym. Chem.* 1979, **20** (2), 528
18 Schmitt, R. L., Gardella, J. A., Magill, J. H., Salvati, L. and Chin, R. L. *Macromolecules* 1985, **18**, 2675
19 Yoon, S. C. and Ratner, B. D. *Macromolecules* 1986, **19**, 1068
20 Green, P. F., Christensen, T. M., Russell, T. P. and Jerome, R. *Macromolecules* 1989, **22**, 2189
21 Bhatia, Q. S., Pan, D. H. and Koberstein, J. T. *Macromolecules* 1988, **21**, 2166
22 Burrell, M. C. and Chera, J. J. *Appl. Surf. Sci.* 1988, **35**, 110
23 Briggs, D. *Polymer* 1984, **25**, 1379
24 Briggs, D. *Surf. Interface Anal.* 1986, **9**, 391
25 Briggs, D. *Br. Polym. J.* 1989, **21**, 3
26 Briggs, D., Brown, A. and Vickerman, J. C. 'Handbook of Static Secondary Ion Mass Spectrometry', Wiley, New York, 1989
27 Hearn, M. J., Briggs, D., Yoon, S. C. and Ratner, B. D. *Surf. Interface Anal.* 1987, **10**, 384
28 Hearn, M. J., Ratner, B. D. and Briggs, D. *Macromolecules* 1988, **21**, 2950
29 Burrell, M. C., Bhatia, Q. S., Chera, J. J. and Michael, R. S. *J. Vac. Sci. Technol.* 1990, **A8**(3), 2300
30 Witsiepe, W. K. 'Polymerization Reactions and New Polymers' (*Adv. Chem. Ser.* **129**), American Chemical Society, Washington DC, 1973
31 Hoeschele, G. K. *Chimica* 1974, **28**, 544
32 Briggs, D. and Seah, M. P. (Eds.) 'Practical Surface Analysis by Auger and X-ray Photoelectron Spectroscopy', Wiley, New York, 1983
33 Burrell, M. C., Bhatia, Q. S. and Michael, R. *Appl. Surf. Sci.* 1991, submitted
34 Wu, S. 'Polymer Interface and Adhesion', Dekker, New York, 1982
35 Gaines, G. L. Personal communication
36 Wegner, G., Fujii, T., Meyer, W. and Lieser, G. *Angew. Makromol. Chem.* 1978, **74**, 295
37 Goldblatt, R. D., Scillia, G. J., Park, J. M., Johnson, J. N. and Huang, S. J. *J. Appl. Polym. Sci.* 1988, **38**, 632
38 Hariharan, A., Kumar, S. K. and Russell, T. P. *Macromolecules* 1990, **23**, 3584
39 Frensdorff, H. K. *Macromolecules* 1971, **4**, 369
40 Clark, D. T. and Thomas, H. R. *J. Polym. Sci., Polym. Chem. Edn* 1977, **15**, 2843
41 Szajman, J., Liesegang, J., Jenkin, J. G. and Leckey, R. G. G. *J. Electron Spectrosc. Relat. Phenom.* 1978, **14**, 247
42 Tyler, B. J., Castner, D. G. and Ratner, B. D. *J. Vac. Sci. Technol. (A)* 1989, **7** (3), 1646
43 Hasegawa, H. and Hashimoto, T. *Macromolecules* 1985, **18**, 589
44 Henkee, C. S., Thomas, E. L. and Fetters, L. J. *J. Mater. Sci.* 1988, **23**, 1685
45 Fredrickson, G. H. *Macromolecules* 1987, **20**, 2535
46 Theodorou, D. *Macromolecules* 1988, **21**, 1422
47 Anastasiadis, S. H., Russell, T. P., Satija, S. K. and Majkrzak, C. F. *Phys. Rev. Lett.* 1989, **62** (16), 1852